82072
PREPRINT UCRL- ~~82764~~

Lawrence Livermore Laboratory

DOES DIAMOND MELT?

R. Grover

June 1, 1979

This paper was prepared for submission to
Journal of Chemical Physics

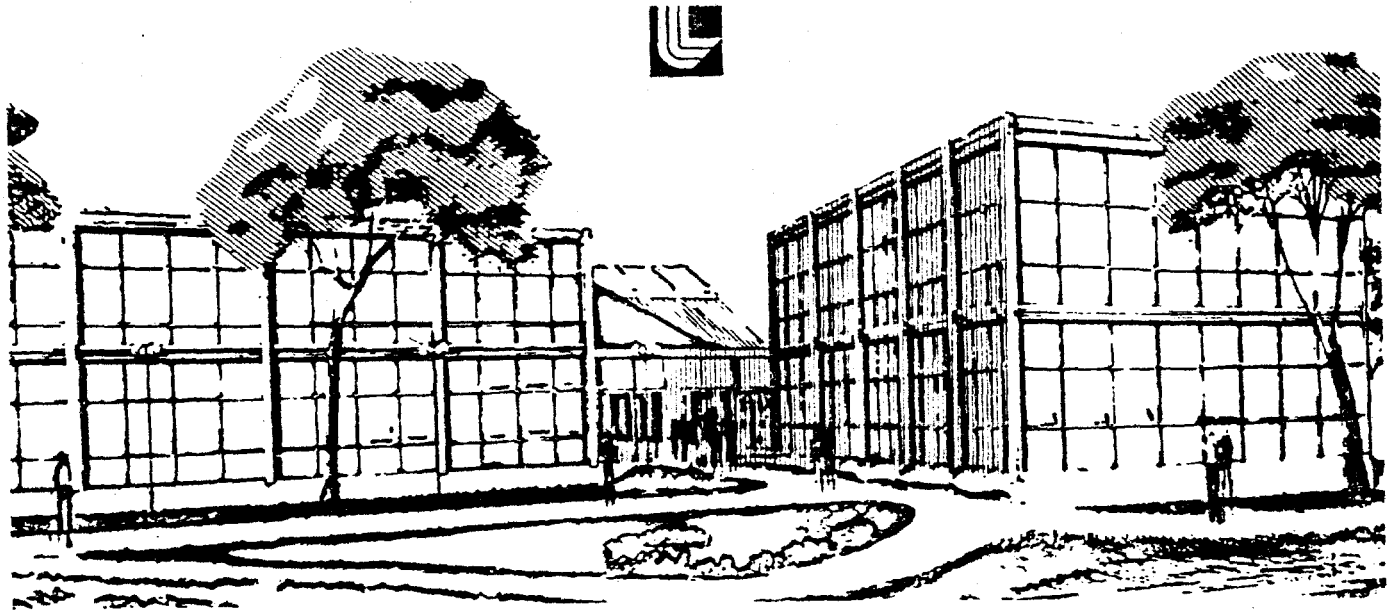

DOES DIAMOND MELT?*

R. Grover
University of California, Lawrence Livermore Laboratory
Livermore, California 94550

Abstract

Recent dynamic compression data for carbon is discussed which suggest that metallic carbon has unexpected thermodynamic properties, both in having a lower density and energy of formation and a higher melting temperature. On the basis of these properties the diamond phase of carbon is now predicted to transform to a solid phase of metallic carbon at all pressures above the graphite triple point.

*Work performed under the auspices of the U.S. Department of Energy by Lawrence Livermore Laboratory under contract #W-7405-Eng-48.

1. Introduction

Although the light group IV elements, C and Si, are expected to transform to metallic-like phases at sufficiently high pressures and/or temperatures, relatively little is definitely known about the temperature-pressure (T-P) boundary for this transition or about the properties of the metallic phases. In addition to their essential role in determining the stability field of the diamond phase, these metallic phases have both technological and geophysical importance, connected primarily with how they will mix with other metallic solids and liquids. For example, in their interstitial compounds with transition metals, C and Si can be viewed as combining with the transition metal in the metallic phase.[1]

Experimental phase diagram data as well as semi-theoretical arguments have been used to predict the extreme parts of the carbon phase diagram. Most recently Van Vechten[2] has made predictions based on scaling the volume changes observed in the corresponding transitions for the group IV and III-V intermetallic compounds and on a simplified dielectric theory for internal energies. For carbon a substantial part of this predicted high temperature boundary of the diamond (α) phase with the metal (β) phase lies adjacent to a liquid phase as illustrated in Figure 1. Although the Van Vechten procedure predicts transition pressures within experimental error for many III-V and II-VI compounds,[2] recent data[3] reveals significant disagreement with detailed predictions of the dielectric theory for these compounds. In the case of carbon the phase diagram predictions must be considered a particularly severe test of the Van Vechten procedure because of the extreme atomic volume and bulk modulus of diamond (relative to the heavier elements) together with the extreme simplifications made in the dielectric theory.

Conventional equilibrium measurements of the thermodynamic properties of carbon in the vicinity of the metal transition are not yet possible because of the high required pressures and temperatures. There is however a variety of experimental evidence for the existence of metallic carbon. Bundy's extensive pulse heating experiments below 20 GPa on the graphite diamond system appear to have located the graphite-diamond-metal (γ-α-β) triple point[4] and constitutes the most direct experimental evidence for the existence of the liquid metallic phase. This experimental triple point at 4000 K and 12.5 GPa is somewhat lower than predicted triple point shown in Figure 1. In addition there is preliminary evidence of reversible changes of state in a diamond cell apparatus at pressures of 170 GPa[5a] and a rapid increase in electrical conductivity of diamond in a high stress "indenter" apparatus at a high but indeterminate stress.[5b] More recently a significant amount of high density dynamic shock compression data on carbon has become available[6-9] and provides further but confusing evidence for the metallic phase. On the one hand single-crystal diamond data provide evidence for the α-β transition within the range of expected transition pressures at low temperature (e.g. see Figure 1). However shock compression data on a variety of forms of graphite appear to rule out the possibility of the expected diamond transition to a dense metallic phase at higher temperatures. More detailed discussions of these data and their interpretation are presented in sections 3 and 4.

In order to resolve this data paradox and to understand its broader implications concerning the properties of carbon at extreme conditions we have made use of a conservative phenomenological equation-of-state (EOS) model for the various solid and liquid phases of carbon. The merits of this model and its application to carbon are reviewed in section 2. After fitting the available data the resulting solid metallic phase of carbon is found to be more stable

then the liquid all along the boundary with the diamond phase. The properties of the metal phase leading to this prediction are theoretically evaluated in the concluding section by a systematic comparison with known metals and with some preliminary electron band-structure calculations. The adequacy of our interpretation of the present data could be tested both by a more extensive and accurate data base of the current type as well as by more novel data as discussed also in section 4.

2. Equation-of-State Modeling

In order to avoid the difficult problem of constructing any kind of reliable microscopic theory for the condensed phases of carbon we have used reasonable phenomenological models for the free energy of all carbon phases whose parameters, it turns out, may be adjusted to fit available experimental EOS data. For instance in the α(diamond) phase an adequate EOS of the quasi-harmonic Grüneisen form can be determined simply from high temperature thermophysical data[10,11] and recent ultrasonic velocity data on single crystal diamond.[6] According to quasi-harmonic theory the thermal free energy, F_{th}, and Grüneisen ratio, Γ_G, are related at high temperature to a Grüneisen characteristic temperature θ_G, defined as the geometric mean lattice frequency, by

$$F_{th} = -3RT \ln (T/\theta_G), \quad \Gamma_G \equiv \frac{d\ln\theta_G}{d\ln\rho} \tag{1}$$

The remaining static contribution to the elastic energy of the lattice can be determined from the measured pressure variation of sound velocities in diamond.[6] For pyrolytic graphite (assumed to adequately represent "single crystal" graphite) shock velocity data[7] can be similarly combined with high

temperature thermophysical data to give a reliable EOS for the γ(graphite) phase of carbon. In this case the Grüneisen coefficient is determined primarily by the behavior of the ratio of thermal expansion coefficient to specific heat at high temperatures. Table 1 contains the EOS parameters used for the γ and α phases of carbon. The parameters in the table from which the elastic energy is derived are the usual shock velocity coefficients in the relationship between shock velocity, D, material velocity, U, for plane shock waves and normal sound velocity C_B,

$$D = C_B + S\,U\,, \qquad S = \frac{1}{4}\,(1+B') \tag{2}$$

We indicate here also how S is related to the rate of change of bulk modulus with pressure, B', as determined from sound velocity data. The static lattice energy is obtained from the Hugoniot $P_H(\rho)$ locus, determined by Eq. (2), after subtracting the thermal energy and pressure derived from Eq. (1). In making this subtraction we have assumed slight linear volume dependence of Γ_G (towards 0 and 0.5 at zero volume respectively for diamond and graphite). When the α phase is assigned an internal energy of 2.4 kJ/gm-at relative to the γ phase (at standard conditions) the 300 K transition γ-α is found by free energy equality to occur at 1.3 GPa and the T-P phase boundary is in close agreement with Bundy's[4] estimated boundary up to the triple point (see Figure 1). We therefore assume that the γ and α phases of carbon behave thermodynamically like normal Grüneisen solids at all T and P of interest.

There are also reasons to expect that, at least thermodynamically, metallic (β phase) carbon may be "normal". For instance the analagous group IV metal, white-tin, has, in spite of its low symmetry, a normal corrected

entropy change at melting, a "normal" specific heat behavior in the liquid phase[12] and satisfies the Lindemann law. A general liquid EOS model having these "normal" properties has previously been formulated[13] on the basis of the properties of low melting point metals and an extensive amount of computer simulation data for many particle systems with pairwise interactions. In this formulation the Lindemann law, expressed most accurately in terms the excess thermal free energy F_{th}^{x} at melting from Eq. 1, can be written in its normal and "compression" form as

$$-\frac{F_{th}^{x}}{RT_M} = 8.074 - \frac{3}{2}\,\ell n\left(\frac{T_M}{A_W V_A^{2/3}\,\theta_G^2}\right) \quad , \lambda \equiv \frac{d\ell nT_M}{d\ell n\rho} = 2\Gamma_G - \frac{2}{3} \qquad (3)$$

$$= 6.05 \pm 0.1$$

Thermal EOS properties in the liquid phase then depend simply on $\tau \equiv T/T_M$, the temperature scaled to the melting temperature characteristic of the density, as derived from an excess specific heat which decreases by a factor of $1 + 0.1\,\tau$ in the liquid phase. The scaling-law EOS model has been successfully applied to experimental data for a variety of metals[13] and in particular to the metallic phase of Si where dynamic shock compression data, high temperature thermophysical data and phase diagram data were fit.[14] On the basis of this experience we feel justified in claiming that the liquid model can be used to represent an average liquid EOS for metallic carbon over a wide range of pressure and temperature.

3. Determination of Metallic Carbon EOS Parameters

There are three types of experimental EOS data on carbon which have been considered independently for evaluating the metallic EOS parameters. Since

this data is limited and intrinsically not of high precision in some cases, the EOS parameters are not conclusively determined. It is therefore appropriate to briefly summarize our modeling procedure.

We first make use of the dynamic compression data, both ultrasonic[6] and shock velocity[8] data on single crystal diamond, which provides direct experimental evidence for the α-β transition. In Figure 2a, the two sets of data are compared in a D-U plot (using C_B and S from Table 1) where the data can be seen to be inconsistent. The discrepancy in the intercept of the shock velocity data with the measured bulk sound speed is $\sim$5 times larger than normal for carefully measured shock data in well characterized material samples. Because of the steeper slope of the ultrasonic data, however, the two sets of data can be combined by assuming there is a bend in D at U = 3.7 km/sec (as indicated by the bar) corresponding to a shock pressure $\sim$ 200 GPa. If the break is attributed to the metallic transition, there are two ways to interpret the linear shock data beyond the break. It can represent the linear D-U relation of the metal phase which is only slightly denser than the diamond phase, or it may lie in a two-phase region of a transition with large $\Delta V/V_0$. The latter possibility corresponds to the Van Vechten model and, because of the large non-equilibrium effects expected in such cases, does not allow any significant thermodynamic information to be extracted from the D-U data beyond the break. However in the former case we have been able to locate a "best" fit to the compressibility properties of the metal phase, β_1, as shown by the first four columns of Table 1. In this search we varied the normal density ρ_0 over the range which permitted the diamond shock data above 2 Mb to be fit by Eq. (2) for the metal phase. For densities greater than the table value, it becomes necessary to add a significant quadratic term to Eq. (2) and for lower densities the metal phase tends to become more stable

than the diamond phase at zero pressure and 300 K. This procedure is not sensitive to the assumed value of Γ_{G0} because the amount of irreversible shock heating in diamond samples is relatively small.

We can next determine the thermal parameters in our metal equation-of-state model, T_{M0} and Γ_{G0}, (θ_{G0} from Eq. (3)) at the reference density, $\rho = \rho_0$, by fitting the second set of data, the pulse heating data in the vicinity of the γ-α-β triple point.[4] Somewhat to our surprise we found in this step that the diamond phase could not be stabilized with respect to the metal near the observed triple point unless a high melting temperature is assumed, in which case it is the solid metallic carbon that is in equilibrium at the experimental triple point. In his experiments on the crystallization of diamond from unalloyed graphite by pulse heating Bundy[4] detected the metal transition in large pulses at pressures above the triple point. He furthermore concluded that the metal phase was likely to be a liquid phase from the appearance of the mixed diamond-graphite cores that are recovered after the experiments. Except for this latter conclusion however which will be further discussed in section 4, the phase boundaries in Figure 1a of metallic carbon, described by the parameters for β_1 in Table 1, are in satisfactory agreement with experimental data. Phase diagram calculations for a variety of thermal parameters show that the calculated triple point is more sensitive to T_{M0} than Γ_{G0}. A choice of 1.1 for Γ_{G0} does not change the triple point significantly.

For comparison we have generated the EOS of a higher density metallic carbon phase, β_V, with a scaling EOS model. With parameters shown in Table 1, the scaling model produces an equilibrium phase diagram in close agreement with Van Vechten's[2] except for unessential differences near the diamond-metal triple points (see Figure 1). As a starting point from which to vary

parameters in the latter search, we scaled our previously discussed EOS model for metallic Si. The differences in these (β_V) parameter values from those of the β_1 model can be readily understood. The high pressure, low temperature transition can be brought about at the same pressure but higher density by increasing its energy of formation, ΔE_0. However to obtain the same graphite triple point with a larger ΔE_0, one must lower the free energy of the metal by lowering its Debye and melting temperatures.

4. Agreement with Low Density Carbon Shock Data

A third source of useful experimental data is the extensive set of shock-compression experiments on various kinds of low density carbon.[7-9] Although these experiments were the first to detect the graphite-diamond transition, they have not been as useful for extracting equilibrium thermodynamic properties of the high density phase because of the large overdriving shock pressures required to induce the graphite transition to diamond.[7] By restricting our attention to the data at very high pressure and temperatures above the graphite transition, we may hope to obtain more reliable thermodynamic data pertinent to the diamond-metal (α-β) transition. Figure 2b shows the recently published data of Gust[9] on three types of graphite. A large scatter is evident in the data for porous Ceylon and synthetic graphite samples which presumably arises from the expected non-uniform density in porous samples.

The comparison between experiment and theory is most clearly made in the experimental velocity plane of Figure 2. For this reason the calculated equilibrium graphite Hugoniots in the vicinity of the α-β transition are shown in Figure 2b for both the high (β_V) and lower density (β_1) metal model. The comparison first appears to tell us that some non-equilibrium effects are

present near the α-β transition, since the transition breaks are not evident and neither metal model (or any suitable interpolation between the two) closely fits all the graphite data.

Secondly, although the α-β_1 transition cannot be explicitly seen for the β_1 model, the data is roughly consistent with an equilibrium transition for Ceylon graphite and overdriven transitions (by 10-15% in shock velocity) for both pyrolytic and synthetic graphites within the range of the data. On the other hand if the β_V model is indeed the real one, the shock data for all three forms of graphite must lie below a very large overdriving stress which is required to initiate the transition on the time scale of shock compression. This appears unlikely however in view of the extremely high diamond temperatures that would be reached at the highest shock stresses (6000-7000 K). It would also appear to be inconsistent with our original assumption that the crystal diamond Hugoniot undergoes a transition at $\sim$ 200 GPa at a much lower shock temperature ($\sim$ 1000 K, see below). We conclude therefore that the graphite shock data strongly favors the lower density, β_1 model for metallic carbon.

A selection of this same graphite data is plotted in the P-ρ plane in Figure 3 together with high pressure shock data on porous carbon samples from several Russian reports. A number of points from the latter sources, which are circled, represent data on very thick samples (1 to 7 centimeters) in which non-equilibrium attenuation of the shock wave (on a μsec time scale) should be minimized.[15] This data confirms the errors in earlier data which was claimed to have indicated the diamond-metal transition.[16] The data sources displayed in Figure 3 appear to be consistent within a large scatter although the theoretical order of the Hugoniots with porosity is barely

visible. The inconsistency of the shock data with the equilibrium Hugoniot for the β_V metal is even more evident.

In order to further clarify the thermodynamic and experimental consequences of our models for carbon metal we have plotted in Figures 1 and 4 the equilibrium phase diagrams for the two metallic carbon models together with the equilibrium Hugoniot paths for various graphs. For instance, note in Figure 1 for the β_V metal that, if the equilibrium Hugoniot was followed by experiment, an unusual lowering of the Hugoniot temperature with pressure would occur as a result of following the phase boundaries. If on the other hand the Hugoniot remains metastably in the diamond phase, as the shock velocity measurements would imply in this case, the Hugoniot temperature should increase steadily while the electrical resistivity would remain high up to the highest pressures. Figure 4 shows the corresponding Hugoniot paths in the phase diagram for the β_1 metal. Shock temperatures here increase smoothly through the phase transition while the electrical resistivity decrease down to the metal range. Pulsed x-ray crystallography may also possibly be able to distinguish between the diamond and metallic phases at the highest shock stresses. Our approach provides no guidance, however, as to which crystal phase (or phases) should be expected. Note that the estimated triple point from GE experiments[4] is close to that calculated for the β_1 metal and that an unobserved nearby second triple point is also predicted. The closeness of the two triple points in both pressure and temperature will make the experimental recognition of the solid phase more difficult. In the GE pulse heating experiments the probable conditions of the sample at maximum temperature were less well determined than in the graphite melting experiments and the presence of graphite in the recovered core was not satisfactorily explained. More experimental data in this region would be of interest. (I am

indebted to Dr. F. P Bundy for both discussion and correspondence on this matter.) On the other hand the closeness of the triple points raises the possibility that relatively small deviations in the thermodynamic properties of the liquid phase from "normal" model behavior, which lower its free energies, might lower the melting line to the α-β transition line.

5. Evaluation of Metallic Models

A fault of our procedure for normalizing the metal EOS so far is that separate groups of parameters (T_{M0}, Γ_{G0}) in the thermal part and (C_B, S, ΔE_0) in the static lattice energy are adjusted independently of each other without any limitations corresponding to the requirement that they be derive-able from the same many-body interactions between carbon atoms. Only in a lowest "fluid continuum" (Debye) approximation to the thermal EOS can these interelationship be simple enough to be tested by our model. In this low approximation there are two relationships which should be approximately satisfied. First if the melting temperature satisfies a Lindemann property, then it should be proportional to the bulk modulus times the atomic volume of the solid. Secondly, the Gruneisen ratio should be related to the pressure derivative of the sound velocity, or, through relation (2), to s. We use a form of the relationship preferred in EOS modeling for metals,[17] the Dugdale-McDonald formula which states that $\Gamma_{G0} = 2S-1$. Since both relations are very approximate we must not expect corresponding ratios to be constants but rather to vary in a small but systematic way through the periodic table. In order to see how consistent our hypothetical constants are in this sense with those of other related metals, we have collected a number of parameters for the second row and group IV metals in Table 2. It can be seen in the Table that, judging by the tabulated quantities, metallic carbon is more

distantly related to its other group IV members than it is to its second row neighbors or than the other group IV elements are to each other. In the second row the trends shown by the melting temperature and gamma ratios slightly favor the β_1 model although the distinction is not large in view of the fluctuations in the tabulated ratios. Note that in Table I we have tabulated $\theta_{D0} \equiv \theta_{G0}/e^{1/3}$ and in Table II compared it with experimental θ_D from low temperature specific heats.

It appears feasible at this time to obtain a reliable theoretical model for the metallic phase of carbon by means of a conventional electron band-structure calculation. As a preliminary step in this direction A. K. McMahan of our laboratory has investigated the bcc and fcc crystal structures of carbon which turn out to be metallic at low pressures. The zero-pressure densities were found to be significantly less than that of diamond, apparently not favoring the high density of the β_V model.

Miedema[1] has successfully utilized a high density carbon model with a very large ΔE_0, like that of the β_V model, to explain the heats of formation of the transition metal carbides. The implications of the lower values of ρ_0 and ΔE_0 of the β_1 model for such alloy models are now under study.

In conclusion it has been demonstrated that experimental EOS data (virtually all "dynamic") favors a metallic phase of carbon characterized by lower densities and higher melting temperatures than had previously been expected. It is perhaps not surprising that strict group-IV scaling should not be followed in this case in view of the exceptionally high atomic density and bulk modulus of carbon. Various experimental methods of distinguishing between these models were outlined based on dynamic methods of measuring temperature, resistivity and crystal structure in shock-wave experiments. The

full predicted EOS of carbon based on fitting the β_1 model to current data is plotted in Fig. 5. It shows a very large stability field for a single solid metallic phase. This single phase should not be taken too literally inasmuch as our β_1 model may represent the average behavior in this field of several metallic or semi-metallic phases with relatively small thermodynamic differences and approximately "normal" melting behavior, as appears to be the case for metallic Sn and some group III-IV compounds.[3]

Acknowledgements

We would like to express our appreciation to Drs. B. Vodar, R. N. Keeler and H. C. Graboske for the opportunity to pursue this research. We would also like to thank Dr. A. K. McMahan for calculations and discussions concerning the electron-band structure of metallic carbon and W. H. Gust for making available the tabular graphite shock data before publication.

Table I

Carbon Phase	ρ_0 gm/cc	C_B cm/μsec	S	ΔE_0 kJ/gm at	θ_{D0} K	Γ_{GO}	T_{M0} K
γ	2.267	.475	1.5	0	1478	.37	—
α	3.51	1.122	1.26	2.4	1850	—	—
β_1	3.75	1.37	1.0	33	1693	1.5	6000
β_V	4.65	1.07	1.4	122	969	1.8	2400

ρ_0 - reference density in standard state (300 K and 1 atm)

C_B - shock velocity parameters to fit to experimental data, $D = C_B + Su$

ΔE_0 - internal energy in standard state of given phase relative to that of the graphite

θ_{D0}, T_{M0}, Γ_{G0} - Debye temperature, melting temperature, and Gruneisen coefficient at reference density, ρ_0

Table II

Metallic Element	V_{A0} (cc/mole)	B_0 (GPa)	θ_{D0} (K)	T_{M0} (K)	Γ_{G0}	$\frac{T_{M0}}{B_0 V_{A0}}$	S	$\frac{\Gamma_{G0}}{2S-1}$
Li	13.02	10.9	352	454	.9	3.20	1.133[a]	0.71
Be	4.89	119	1160	1557	1.15	2.68	1.124[a]	0.92
B	4.66	183	1315	2498	1.4-1.8	2.93	—	—
$C\beta_1$	3.20	700	1693	6000	1.5(1.1)	2.68	1.0	(1.1)
$C\beta_V$	2.58	534	969	2400	1.8	1.74	1.4	1.0
$Si\beta$*	9.06	67	350	900	2.2	1.48	1.4	1.22
$Sn\beta$	16.30	55	195	505	2.1	0.56	1.486[a]	1.06
Pb	18.27	45	119	600	2.7	0.73	1.46[a]	1.41

a - Data of GMX-6 group, LASL (LA-4167-MS, 1969, unpublished).

V_{A0} - atomic volume

B_0 - bulk modulus in standard state

* - from ref. 14

References

1. A. R. Miedema, J. Less-Common Met. 46, 67 (1976).
2. J. A. Vechten, Phys. Rev. B7, 1479 (1973).
3. S. C. Yu, I. L. Spain, and E. F. Skelton, Solid State Comm. 25, 49 (1978).
4. F. P. Bundy, J. Chem. Phys. 38, 631 and 618 (1963).
   F. P. Bundy, H. M. Strong, and R. H. Wentorf, Jr., Chem. and Phys. of Carbon 10, 213 (1973).

5a. H. K. Mao and P. M. Bell, Science 200, 1145 (1978).

b. L. F. Vereshchagin, E. N. Yakovlev, G. N. Stepanov, and B. V. Vinogradov, Sov. Phys.-JETP.

6. H. J. McSkimmon and P. Andreatch, J. Appl. Phys. 43, 2944 (1972).
7. R. G. McQueen and S. P. Marsh, Proceedings of Symposium on High Dynamic Pressures (1967), Paris, France (Gordon and Breach, New York, 1968).
8. M. N. Pavlovskii, Sov. Phys.-Solid State 13, 741 (1971).
9. W. L. Gust and D. A. Young, High Pressure Science and Technology, (K. D. Timmerhaus and M. S. Barber, ed.), p. 944, vol. 1 (Plenum Press, New York, 1979).
10. R. Hultgren, P. D. Desai, D. T. Hawkins, M. Gleiser, K. K. Kelley and D. D. Wagman, Selected Values of Thermodynamic Properties of the Elements, (American Society of Metals, Metals Park, Ohio, 1973).
11. American Inst. Physics Handbook, 3rd Ed. (McGraw-Hill, New York, 1972), section 4e.
12. R. Grover, J. Chem. Phys. 55, 3435 (1971).
13. R. Grover, Proceedings of 7th Symposium on Thermophysical Properties (A. Cezairliyan, ed.), p. 67 (Amer. Soc. of Mech. Eng., United Engineering Center, New York, 1977). R. Grover, p. 33 in reference 9.

14. R. Grover, (H-Division Quarterly Report, UCRL-50028-78-3, Lawrence Livermore Laboratory, Livermore, CA 94550, unpublished).

15. M. N. Pavlovskii and V. P. Drakin, Sov. Phys.-JETP Lett. 4, 116 (1966).

16. B. J. Alder and R. H. Christian, Phys. Rev. Lett. 7, 367 (1961).

17. M. H. Rice, R. G. McQueen and J. M. Walsh, Solid State Phys. 6, 1 (1958).

Figure Captions

Fig. 1 Carbon temperature-pressure phase diagram for a high density metallic phase (β_V). Hugoniot temperatures for various types of low density carbon: s—synthetic graphite, d—porous diamond, c—Ceylon graphite, p—pyrotylic graphite. Experimental triple point—O. Solid and liquid metallic phases are indicated by β_s and β_ℓ.

Fig. 2a Dynamic compression data for single crystal diamond:

diamond shock (D) vs particle (u) velocity data—O,

ultrasonic velocity data—line through the bulk sound speed "C_B"

intersection— ⊢—⊣

Fig. 2b Comparison of graphite shock velocity data with model calculations. For visual clarity solid lines have been drawn through the graphite data (⊙, △, ⊡). β_1 and β_V indicate model velocity calculations.

p—calc. Hugoniot for pyrolytic ($\rho_0 \simeq 2.26$ gm/cc)

C—calc. Hugoniot for Ceylon ($\rho_0 \simeq 2.16$ gm/cc)

S—calc. Hugoniot for synthetic ($\rho_0 \simeq 1.78$ gm/cc)

Fig. 3 P-ρ graph of high pressure carbon shock data:

S—synthetic graphite, p—pyrolytic graphite, t(TP)—α-β_1 transition

$P_{0\alpha}$—extrapolated ultrasonic compression curve

$P_{0\alpha_1}$—extrapolated β_1 metal compression curve

———Hugoniots for β_1 metal phase, showing diamond metal and melting transitions

— —the same for β_V metal phase showing diamond-metal transition

Fig. 4 Carbon temperature—pressure phase diagram for the β_1 model of metallic carbon. See Fig. 1 for notation. Two triple points, t_1 (T,P) and t_2 (T,P), between graphite, diamond, and/or metallic carbon are predicted.

Fig. 5 Pressure EOS surface for carbon predicted with β_1 metallic carbon. Same notation as Fig. 1. Crystal diamond Hugoniot indicated by x.

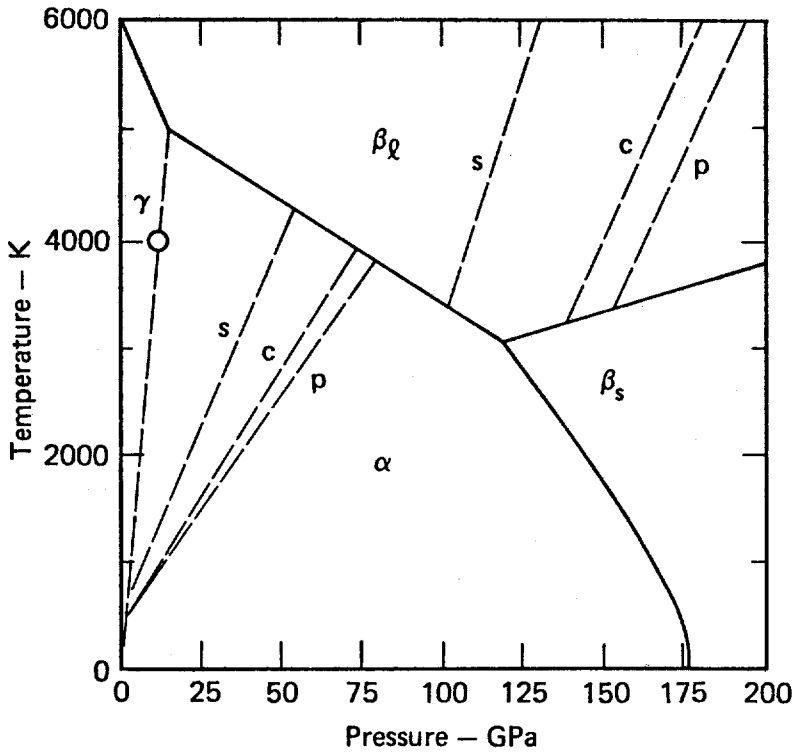
6000
4000
2000
0
Temperature – K
0
25
50
75
100
125
150
175
200
Pressure – GPa
β_ℓ
s
c
p
γ
s
c
p
α
β_s

Figure 1

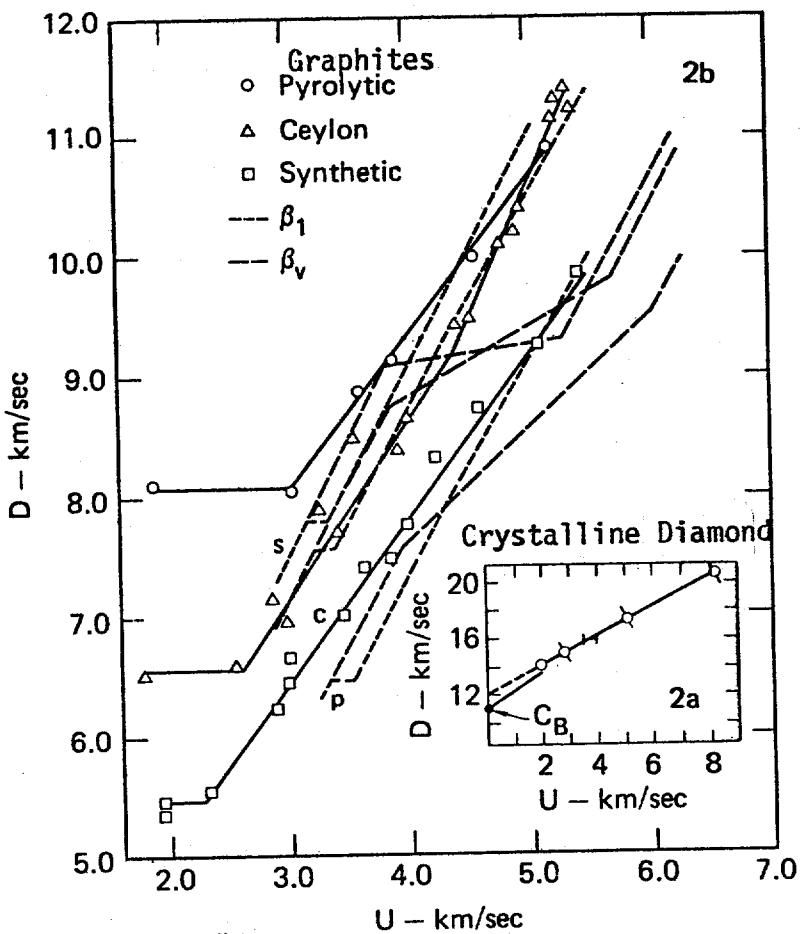
Graphites
Pyrolytic
Ceylon
Synthetic
β_1
β_v
2b
s
c
p
Crystalline Diamond
2a
C_B
D – km/sec
U – km/sec
12.0
11.0
10.0
9.0
8.0
7.0
6.0
5.0
2.0
3.0
4.0
5.0
6.0
7.0
20
16
12
2
4
6
8

Figure 2

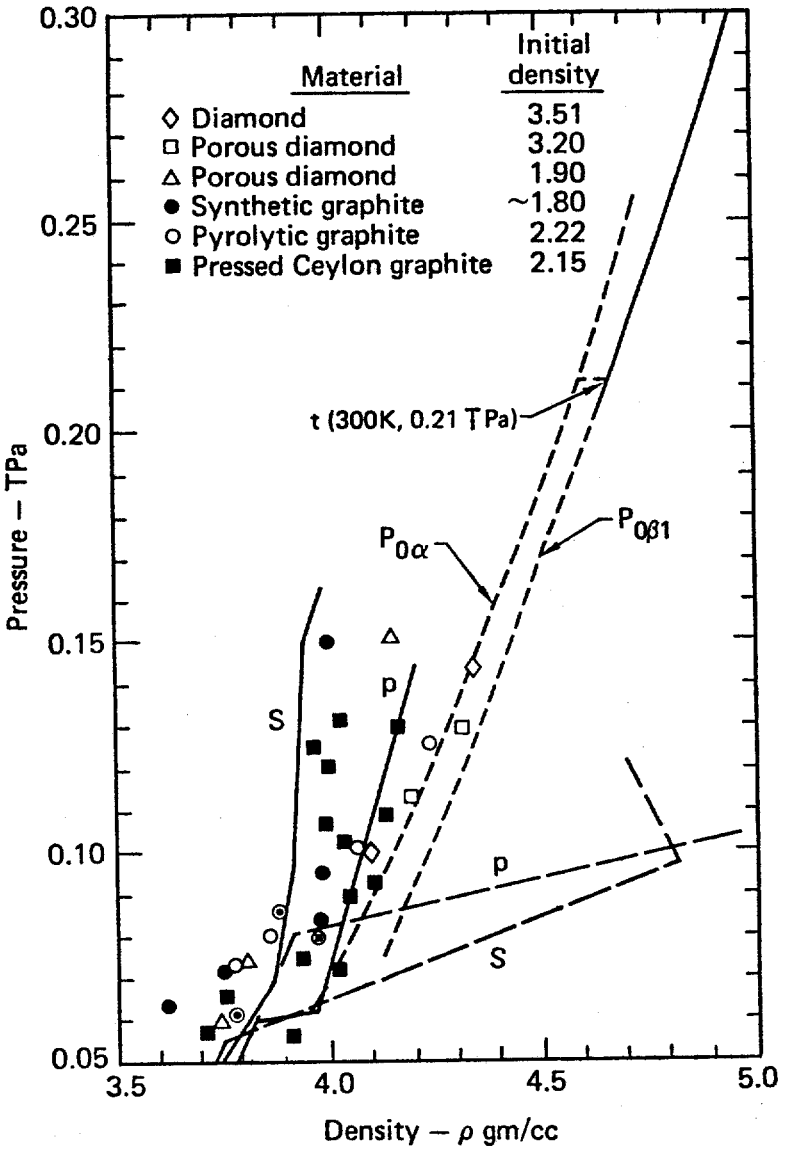
Material
Initial density
◇ Diamond 3.51
□ Porous diamond 3.20
△ Porous diamond 1.90
● Synthetic graphite ~1.80
○ Pyrolytic graphite 2.22
■ Pressed Ceylon graphite 2.15
t (300K, 0.21 TPa)
$P_{0\alpha}$
$P_{0\beta1}$
S
p
p
S
0.30
0.25
0.20
0.15
0.10
0.05
3.5
4.0
4.5
5.0
Pressure — TPa
Density — ρ gm/cc

Figure 3

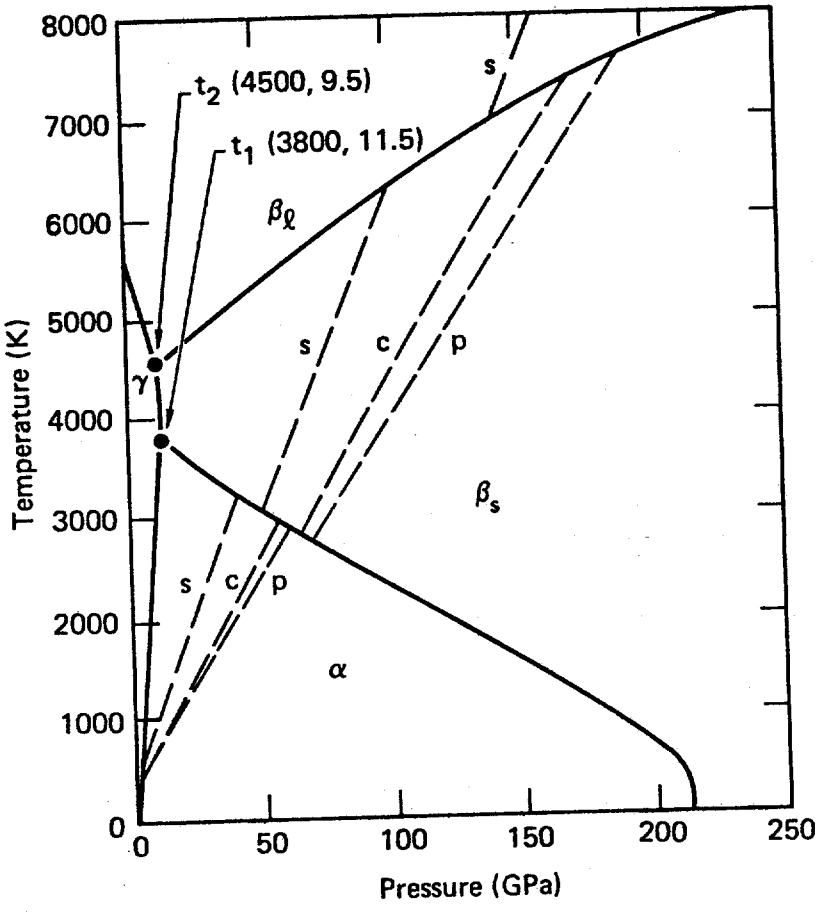
8000
7000
6000
5000
4000
3000
2000
1000
0
Temperature (K)
0
50
100
150
200
250
Pressure (GPa)
t_2 (4500, 9.5)
t_1 (3800, 11.5)
β_ℓ
γ
β_s
α
s
c
p

Figure 4

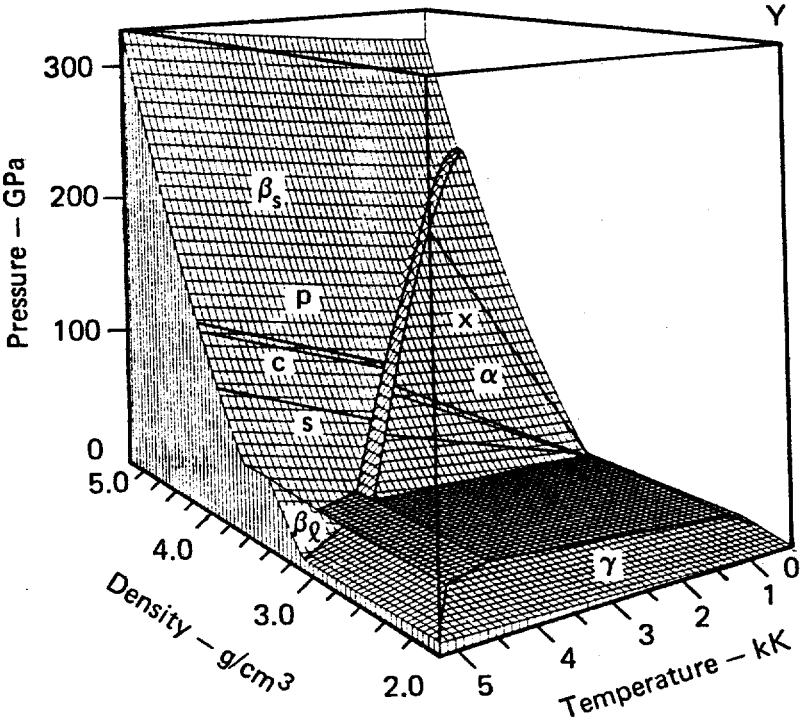
Y
300
200
100
0
Pressure – GPa
β_s
p
c
s
x
α
β_Q
γ
5.0
4.0
3.0
2.0
Density – g/cm3
0
1
2
3
4
5
Temperature – kK

Figure 5

DISTRIBUTION:

R. GROVER, L-355	10
TID, L-52	15